Volume 3
Number 1
January 2026
Pages 1–132

RSC Mechanochemistry

rsc.li/RSCMechanochem

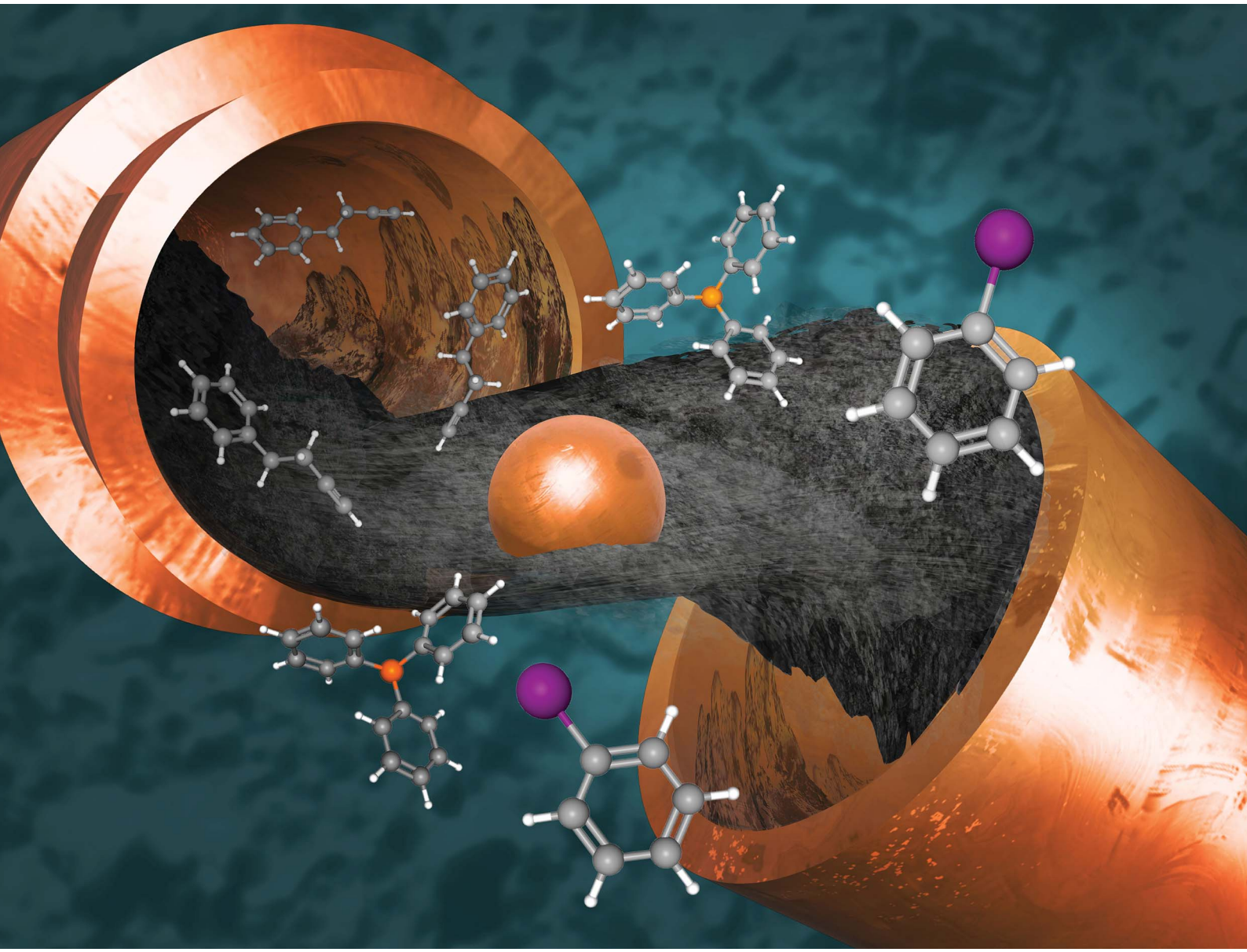

ISSN 2976-8683

ROYAL SOCIETY OF CHEMISTRY

PAPER

James Mack *et al.*

Scratching beneath the surface: catalyst evolution and reusability in the direct mechanocatalytic Sonogashira reaction

RSC Mechanochemistry

ROYAL SOCIETY OF CHEMISTRY

PAPER

View Article Online
View Journal | View Issue

Cite this: *RSC Mechanochem.*, 2026, **3**, 46

Scratching beneath the surface: catalyst evolution and reusability in the direct mechanocatalytic Sonogashira reaction

Sheeniza Shah,[a] Mennatullah M. Mokhtar,[a] Thinh Tran,[a] Kathleen Floyd,[b] Lizette Mella,[b] Tim Dao,[a] Alexandria Garza,[a] James Batteas[bc] and James Mack*[a]

Received 2nd May 2025
Accepted 30th September 2025

DOI: 10.1039/d5mr00060b

rsc.li/RSCMechanochem

We present a solvent-free Sonogashira coupling of various *para*-substituted aryl halides with terminal alkyne using a palladium catalyst and copper (0) co-catalyst under mechanochemical conditions. This study investigates the critical components required for C–C bond formation and explores the *in situ* generation of an active catalyst from individual precursors traditionally used in solution-phase chemistry. We demonstrate the role of palladium [Pd (0)] in different metal forms (powder and foil) within a copper milling jar, highlighting the importance of thermal activation and ligand presence in generating a reactive catalytic species. Notably, Pd was found to embed into the copper surface, enabling multiple reaction cycles without additional Pd, as confirmed by surface analysis. Furthermore, thermal control of the reaction allows for chemoselective activation of one halide over another. Our findings provide insights into the development of catalytic systems during mechanochemical reactions from individual components, offering a cost-effective and sustainable approach to solvent-free organic transformations. This study underscores the potential of mechanochemical methods for designing reusable catalytic systems with enhanced efficiency and selectivity.

1 Introduction

C (sp)–C (sp^2) coupling reactions are crucial for the synthesis of alkyne derivatives utilized broadly across the organic, organometallic, industrial, materials, agricultural, medicinal, and biological chemical industries.[1–3] The classic Sonogashira reaction employs high temperature reflux with stochiometric base in the presence of palladium or copper/palladium bimetallic catalysts to achieve bonding between alkynes and aryl halides or pseudohalides as the electrophilic coupling partners (see Scheme 1).[2,4,5] Recent explorations have advanced this protocol to include reactions with electrophilic diaryliodonium salts, aryldiazonium salts, aryl/benzylic ammonium salt, diaryl sulfoxide, aryl sulfonium salt, and tetraphenylphosphonium.[1] While incredibly beneficial, the standard protocol has a number of drawbacks including reliance on precious metals, air free conditions, high temperatures, and dependence on large amounts of hazardous solvent.

Recent efforts by chemists have been geared to overcoming these limitations. Particularly notable advances have come in the areas of photochemistry and mechanochemistry. Photochemistry has enabled several Pd-free coupling transformations with moderate to good yields.[4] However, the protocols still generally rely on air-free conditions to optimize output and require large amounts of solvent, long reaction times, and high temperatures.[4] In contrast, recent mechanochemical protocols have shown promise to conduct solvent-free Songashira couplings under ambient atmosphere at room temperature with good to excellent yields; but continue to rely on classic copper/palladium bimetallic catalysts to achieve high conversions.

Mechanochemists have responded to the remaining challenge of the metal catalyst by exploiting the unique nature of the solvent free environment. This can be achieved by two main routes. One approach focuses on reducing the amount of precious metal required due to the enhanced relative catalyst concentrations that can be achieved when solvent is removed.[6,7] Alternatively, milling materials in their native metal forms can be employed as the catalysts directly (a technique known as

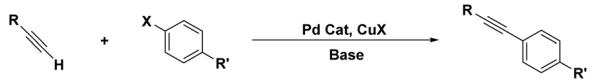

Scheme 1 Sonogashira reaction.

[a]*Department of Chemistry, University of Cincinnati, Cincinnati, OH 45221, USA. E-mail: mackje@ucmail.uc.edu*

[b]*Department of Chemistry, Texas A&M University, College Station, TX 77842-3012, USA. E-mail: batteas@chem.tamu.edu*

[c]*Department of Materials Science and Engineering, Texas A&M University, College Station, TX 77842-3012, USA*

direct mechanocatalysis) thus removing the need for the often complex pre-synthesis of metal–ligand catalyst systems and simplifying catalyst removal and reuse.[7,8] This can include adding ligands to prepare the active catalysts *in situ*.[7,9] These mechanocatalytic techniques have shown promise for a number of reaction systems including cyclopropanations,[10–12] sulfonylurea couplings,[13] cycloadditions of alkynes,[14] Suzuki–Miyaura couplings,[15–17] Glaser couplings,[18] Buchwald–Hartwig reactions,[19–21] CuACC reactions,[22] and Songashira couplings.[6–8,20,23–25] Mechanocatalysis has been particularly well demonstrated for Songashira coupling reactions by the use of Pd and Pd-electroplated milling balls in PFA vials by the Borchardt group.[8,9,24] Their recent explorations have revealed the critical role played by ligands in the reaction system and have demonstrated a Cu-based catalyst complex which differs from the known catalyst complexes expected from traditional solution based protocols.[8]

Previous work in our group has demonstrated that using a copper vial as the milling jar is crucial for the success of this protocol in the presence of a Pd catalyst.[7] In the absence of copper, the reaction did not proceed. This approach can be seen as a complementary inverse to the work of Borchardt and co-workers, where Pd(0) metal acts as the milling material and copper is introduced as a ligated additive (see Scheme 2).[8] Building off this work, we extend our previous explorations along with our recently developed capacity to control the reaction temperature to further develop the Sonogashira coupling reaction examining the applicability of using both elemental Cu milling media and elemental palladium. We demonstrate the selective embedding of Pd powder on the surface of copper vials, enabling C–C bond formation across multiple reaction cycles. This approach allows the system to be recharged with a small amount of Pd powder while a portion remains embedded on the surface. Surface analysis confirms the presence of Pd on Cu, highlighting the role of thermal energy, mechanical mixing, and ligand selection in generating a reactive catalytic species *in situ* for Sonogashira coupling. Furthermore, precise temperature control under solvent-free conditions is achieved using a heating apparatus equipped with a thermocouple attached directly to a heating sleeve enclosing the milling media (see SI 1.2). In combination with ligand variations, this setup enables the chemoselective activation of one halide over another which is a level of selectivity not commonly observed in conventional solution-phase reactions.

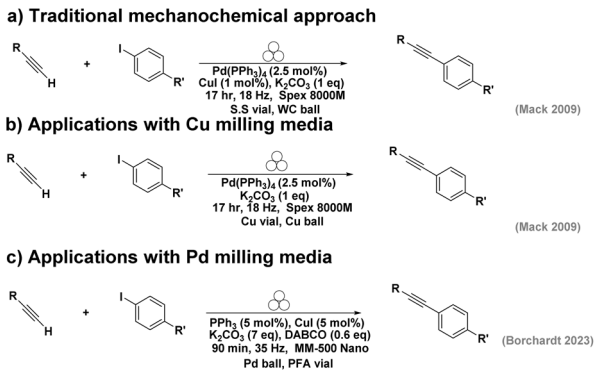

Scheme 2 Explorations of the Sonogashira reaction driven by direct mechanocatalysis.

2 Experimental

All terminal alkynes were purchased from Sigma-Aldrich and used without further purification. Similarly, iodobenzene (98%, Acros Organics), potassium carbonate (Mallinckrodt), caesium carbonate (99%, Acros Organics), and deuterated chloroform (Cambridge Isotope Laboratories, Inc.) were obtained directly from suppliers and used without further purification.

2.1 Nuclear magnetic resonance

^{1}H Nuclear Magnetic Resonance (NMR) spectra were obtained using a Bruker Advance 400 MHz spectrometer. ^{13}C NMR spectra were recorded at 100.6 MHz on a Bruker AV400 spectrometer. Chemical shift values are reported in ppm on the δ scale.

2.2 Flash column chromatography

Flash column chromatography was performed using a Combiflash® Automated Flash Column Chromatography system with RediSep Rf Gold® high performance flash columns (fine spherical silica gel 20–40 μm).

2.3 Gas chromatography mass spectroscopy

Mass spectral determinations were obtained using a Hewlett–Packard 6890 series GC column (30 m, 0.250 mm, 0.25 μm) from J&W GC Columns, sold by Agilent. The samples were analysed using Agilent Technologies 7890B GC/5977A MSD.

2.4 Milling system modifications for direct mechanocatalysis under controlled temperature

All Sonogashira coupling reactions by mechanochemical ball milling were carried out in a SPEX 8000M Miller/Mill operating at a frequency of 18 Hz using a custom-made copper vial with copper shot. Further details on copper and palladium material suppliers and manufacturing are available in SI 1. The heating apparatus used for control of the milling temperature employed is described in detail in previous work[26] (See SI 1.2).

2.5 Scanning electron microscopy (SEM) and energy dispersive X-ray spectroscopy (EDS)

Cleaning and cutting processes to prepare Cu vial samples for subsequent analysis are described in more detail in SI 1. Scanning electron microscopy measurements on Cu vial samples were obtained at the Materials Characterization Facility of Texas A&M University (RRID:SCR_022202) on a Tescan FERA-3 Model GMH Focused Ion Beam Microscope equipped with a Schottky Field Emission electron source, SE and BSE detectors, and an Integrated Plasma Ion Source (Xe) Focused Ion Beam (FIB). An Oxford Ultim Max system was employed for EDS measurements. Beam parameters were as follows: $h\nu = 20$ kV and beam intensity = 15 kV.

2.6 X-ray photoelectron spectroscopy (XPS)

XPS data were obtained using an EnviroESCA (SPECS Group) operating under traditional high vacuum pressure ($\sim 10^{-5}$–10^{-6} mbar). Spectra were processed and fit with peak models developed by Biesinger *et al.*[27] Samples of the Cu vials examined were kept under nitrogen except when loading them into the instrument for analysis (~1–3 min process, an insufficient time for significant oxide formation). To ensure that the potential effects of reduction of the copper surface by X-rays were minimized, Cu $2p^{3/2}$ and Cu LMM (Auger electron spectrum that arises from the electronic transitions within the L shell of an atom) spectra were recorded first, followed by the collection of other XPS data.[26]

3 Results and discussion

3.1 Optimizing Cu (0) and Pd (0) sources as mechanochemical catalysts

Traditional palladium catalysts have many drawbacks including cost, sensitivity, limited shelf life, and different reactivity depending on the supplier.[28] Furthermore, palladium catalysts are generally reacted under inert atmosphere and tend to be difficult to recover. We sought to expand our previous methodology to overcome these challenges by exploring the combination of Pd foil in Cu vials. Foil was chosen as we have previously had success employing direct mechanocatalysis with a number of foil coated vials and it offers high recyclability.[12] The reaction between iodobenzene and 4-phenyl-1-butyne was chosen for initial explorations. When tetrakis(triphenylphosphine)palladium (0) was utilized as the palladium source (in accordance with the established methodology in literature),[7] we routinely observed high yields. Unfortunately, replacing this catalyst with palladium foil only afforded us trace amounts of product and recovered starting materials after 17 h of milling (Scheme 3).

The Stolle group has shown these reactions can proceed much faster in planetary mills using zirconia jars.[6] Planetary mills can operate at temperatures around 120 °C; this is significantly hotter than the shaker/vibratory mills which we are using for our experimental study.[29] More recently the Borchardt group demonstrated the ability to conduct both Sonogashira and Suzuki–Miyaura reactions in a vibratory mill, but needed to shake the vial at 35 Hz to achieve high yields of product.[8,9] These setups also employed larger milling vessels which may enable greater reaction mixing and correspondingly more frictional heating for faster rates. Based on these reports we decided to heat the reaction to determine if the Sonogashira reaction would produce more of the desired product with increased temperature. Unfortunately, we discovered that heating the reaction at 90 °C for 3 hours in the absence of the proper ligand did not improve the reaction yield in the presence of Pd foil.

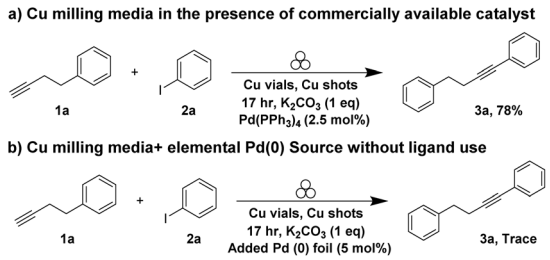

Scheme 3 Comparison of the mechanochemical Sonogashira reaction using different Pd sources: (a) tetrakis(triphenylphosphine)palladium (0) as the palladium source, (b) Pd (0) foil as the Pd source in absence of ligand. The reaction was conducted in a Spex Certiprep 8000M mill.

Such poor yields suggest that performing the reaction with only the native metals is not a feasible process. This is parallel to the findings from the Bolm group when attempting to drive transformations directly with copper and vanadium mineral ores.[30] They observed that adding ligands to convert the minerals to more active forms *in situ* would activate the mechanochemical process.[30] We thus wondered if this would be valuable for our system and found there is warrant for such an approach. Tetrakis(triphenylphospine)palladium (0), first reported in 1957,[31] has been demonstrated to be a very versatile and effective catalyst for a plethora of reactions.[32] It has been demonstrated that mechanochemical conditions inherently mimic the inert reactions conditions needed to perform air and moisture sensitive reactions.[33–35] Because we would be generating the catalyst *in situ*, there would be no need to store the active catalyst. Furthermore, the synthesis of tetrakis(triphenylphospine)palladium (0) requires the use of various harmful reagents which would be avoided under these conditions.[36] This approach also leads to significant savings; 1 gram of tetrakis(triphenylphospine)palladium (0) costs $ 119.5 (USD).[37] The same raw components (*i.e.*, elemental palladium and triphenyl phosphine) that would net a gram of $Pd(PPh_3)_4$ would cost $36.75 (USD).[37–39] Therefore, the net difference of $82.75 $gram^{-1}$ (USD) (69% of the total cost) is related to the cost of assembly and isolation.

Toward this end, we added 10 mol% of triphenylphosphine to the reaction vial, in addition to palladium metal foil and observed a 55% yield after 17 h of milling (Fig. 1). Next, we pursued heating the reaction mixture to reduce reaction times and found that conducting the reaction for 3 hours at 90 °C result in quantitative yield (see Fig. 1 and SI 2). Percent yield was found to be linearly related to temperature (see Fig. 1 and SI 2). Although we achieved high yields in a relatively short time, recovering the palladium foil proved challenging. The foil fragmented into smaller pieces due to abrasion, making it difficult to retrieve (*i.e.*, 100% recovery before triphenylphosphine addition, 60% after), which was a key objective of the experimental design (see SI 3).

Since the recovery of bulk foil was largely unsuccessful, we explored an *in situ* catalyst synthesis using Pd powder instead. This approach aimed at minimizing palladium loss compared to the foil method. Under these conditions, using a large excess of Pd powder (matching the excess available with foil trials) resulted in a 99% yield of the expected coupling product (Table 1, entry 1). However, decreasing the Pd loading led to reduced yields (Table 1, entries 2–4). Interestingly, yield improvements were observed when potassium carbonate was replaced with cesium carbonate (Table 1, entries 5–8 and SI 4).

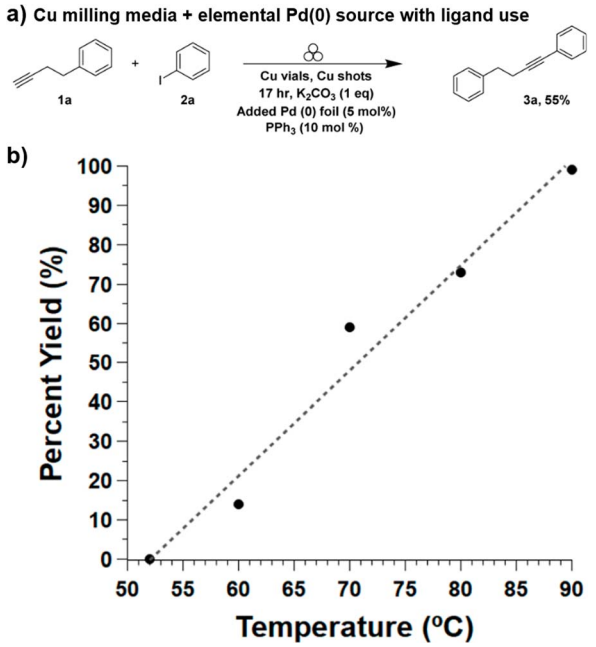

Fig. 1 (a) Mechanochemical Sonogashira using elemental palladium foil and triphenylphosphine at milling temperature (45 °C) and 17 hours of milling. (b) Mechanochemical Sonogashira using elemental palladium foil at various temperatures after 3 hours of milling.

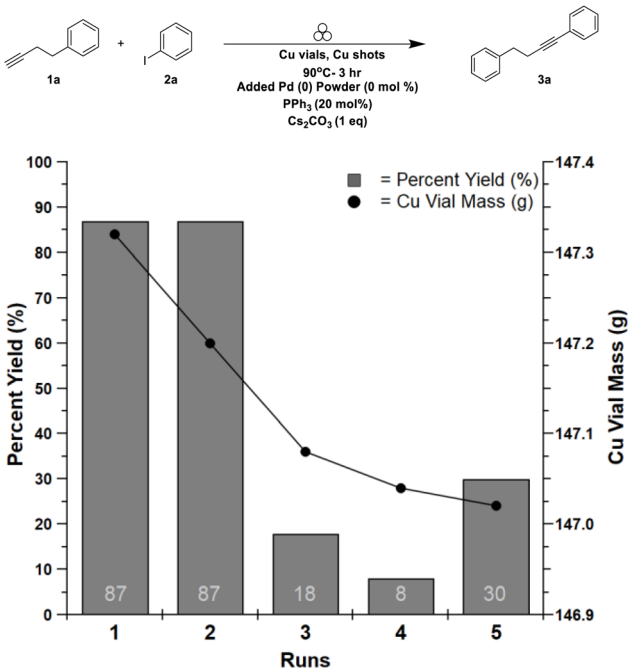

Fig. 2 Recyclability of palladium embedded in copper vial. Replicate reactions performed using a Cu ball (3/32″), Cu vial (2″ × 0.5″) with 3 hours of milling at 18 Hz and 90 °C using a Spex Certiprep 8000M.

Table 1 Sonogashira reaction under optimized conditions using Pd powder and different bases[a]

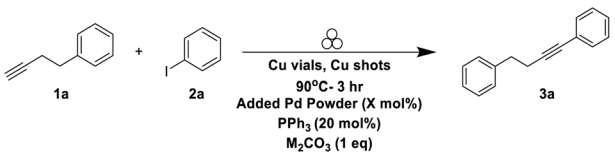

Entry	Added Pd (mol%)	M_2CO_3	Isolated yield (%)
1	230	K_2CO_3	>99
2	5	K_2CO_3	41
3	1	K_2CO_3	53
4	0	K_2CO_3	52
5	230	Cs_2CO_3	>95
6	5	Cs_2CO_3	93
7	1	Cs_2CO_3	90
8	0	Cs_2CO_3	86

[a] Reactions performed using a Cu ball (3/32″), Cu vial (2″ ×× 0.5″) with 3 hours of milling at 18 Hz and 90 °C using a Spex Certiprep 8000M.

Using Cs_2CO_3 with excess Pd powder afforded a 95% yield (Table 1, entry 5), while reducing Pd loading still provided comparable yields (Table 1, entries 6 and 7). Trials exploring alternate ligands for Pd-catalyst generation confirmed that the triphenylphosphine continues to have the best overall reactivity under our conditions (see SI 5). Surprisingly, even in the absence of added Pd powder, the reaction proceeded with an 86% yield (Table 1, entry 8). This result was unexpected, as palladium has traditionally been essential for the mechanochemical Sonogashira coupling. A similarly incongruent outcome was observed when no Pd powder was added in the presence of K_2CO_3 (Table 1, entry 4).

Skeptical of these findings, we repeated the reaction five times under standard conditions without adding new palladium powder. Over these runs, the product yield progressively declined from 86% to 30% (Fig. 2). These results suggested that residual palladium might have embedded itself in the vial walls and was not completely removed by routine cleaning. To test this hypothesis, we machined a new copper vial free of palladium contamination. In this vial, **1a**, **2a**, triphenylphosphine, caesium carbonate, and a copper ball were added under our optimized conditions and milled for 3 hours at 90 °C. Only starting materials were recovered, indicating that the unexpected reactivity observed in our previous experiments (Table 1, entries 4 and 8) was likely due to palladium embedded in the original copper vial.

To minimize powder loss while maintaining high yields, we chose to proceed with the use of 5 mol% Pd for each trial, which was the lowest reliable palladium powder loading to give greater than 90% yield (Table 1, entry 6). In this way we would maintain sufficient Pd loading in the vial to probe the synthetic utility of the process to evaluate the capability of utilizing bulk metals directly rather than catalyst precursors.

3.2 Examining the synthetic utility of catalyst generation *in situ*

We proceeded to investigate the versatility of the palladium-catalysed mechanochemical Sonogashira reaction with various

terminal alkynes under optimized conditions (Table 2). These conditions provided moderate to excellent yields of a variety of alkyne substrates. Excellent yields were observed when 4-phenyl-1-butyne (**1a**), phenylacetylene (**1b**), 1-bromo-4-ethynlbenzene (**1c**), 1-ethynylcyclohex-1-ene (**1d**), were used as substrates (Table 2). Trimethylsilyl acetylene (**S-1a**) provided poor yields at 90 °C, and without any additional heat at long milling times (see SI 6). Since trimethylsilyl acetylene (**S-1a**) has a relatively low boiling point, it is a less effective coupling partner at elevated temperatures. Further, since we observed no cross-coupling product if the reaction is not heated to at least 60 °C (a temperature above the boiling point of trimethyl silyl acetylene) this substrate was not compatible with these conditions. However, using triethylsilyl acetylene (**1e**) provided 67% yield using our optimized conditions (Table 2).

No reaction was observed when propargyl alcohol (**S-1b**) was used as the starting alkyne, most likely due to the alcohol moiety competing with the triphenylphosphine for the palladium (see SI 6). Surprisingly, 1,3-diethynylbenzene (**1f**) only yielded the monosubstituted product (**3f**), exclusively, in 71% yield after 3 hours of milling (Table 2). To obtain the disubstituted product (**3g**), the reaction time was extended to 6 hours, and an additional aryl halide (**2b**) can be used to give product in >95% yield (Table 2).

We then proceeded to investigate other aryl and alkyl halides as coupling partners. We first attempted to substitute iodobenzene (**2a**) with iodododecane (**S-2a**) to observe if our system could tolerate an alkyl halide in hopes of demonstrating a method for forming a sp^2–sp^3 carbon–carbon bond as typical formation requires the use of excess protecting groups and harsh reagents. Unfortunately, only starting material was observed (see SI 6). All other halogens and triflates gave moderate to poor yields (**S-2b**–**S-2d**) (see SI 6). This is unsurprising as such molecules are generally found to be challenging to react in literature.[6,8]

We were able to overcome this limitation in the case of the Aryl bromide substituent (**2c**). While the previous optimized conditions gave only a 2% yield, this value could be increased to 57% by employing excess palladium and higher temperatures (Table 3, entries 1 and 2). While this was promising, we wanted to further reduce the palladium requirements for these substituents. We found that substituting triphenylphosphine with tri-*tert*-butylphosphine provided higher yields for bromide substrate than iodide substrate (Table 3, entries 3–5). A good yield of 84% was obtained when the reaction was conducted at 120 °C for 17 hours (Table 3, entry 6).

Since iodobenzene (**2a**) and bromobenzene (**2c**) are both active at different temperatures and with different ligands, it is quite possible to chemoselectively react one over the other. We demonstrated this by first reacting 1-bromo-4-iodobenzene (**2b**) with phenylacetylene (**1b**) in the presence of triphenylphosphine at 90 °C. This presumably afforded 4-bromo diphenylacetylene (**3c**) as an intermediate with % conversion

Table 2 Various substrates screening for the mechanochemical Sonogashira reaction[a]

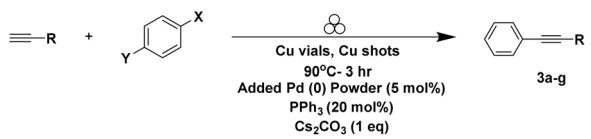

Alkyne (R)	Aryl halide (X,Y)	Product	Isolated yield (%)
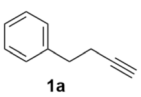 1a	**2a** (I,H)	**3a**	93
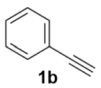 1b	**2a** (I,H)	**3b**	>95
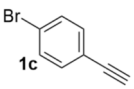 Br 1c	**2a** (I,H)	**3c**	90
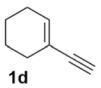 1d	**2a** (I,H)	**3d**	68
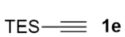 TES 1e	**2a** (I,H)	**3e**	67
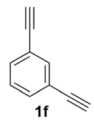 1f	**2a** (I,H)	**3f**	71[b]
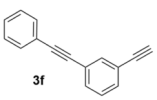 3f	**2b** (Br, I)	**3g**	>95[c]

[a] Reactions performed using a Cu ball (3/32″), Cu vial (2″ × 0.5″) with 3 hours of milling at 18 Hz and 90 °C using a Spex Certiprep 8000M. [b] Mono-addition product observed. [c] Di-addition product made when **1f** was reacted firstly with **2a** and then **2b**.

Table 3 Optimizing conditions for Sonogashira reaction with bromine substituent[a]

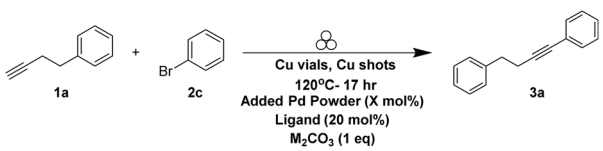

Entry	Added Pd (mol%)	Time (h)	Ligand	M_2CO_3	Isolated yield (%)
1	5	3	PPh_3	K_2CO_3	5
2	230	3	PPh_3	K_2CO_3	57
3	5	3	PPh_3	Cs_2CO_3	5
4	5	3	PCy_3	Cs_2CO_3	3
5	5	3	$P(t\text{-Bu})_3$	Cs_2CO_3	27
6	5	17	$P(t\text{-Bu})_3$	Cs_2CO_3	84

[a] Reactions performed using a Cu ball (3/32″), Cu vial (2″ × 0.5″) with milling at 18 Hz and 120 °C using a Spex Certiprep 8000M.

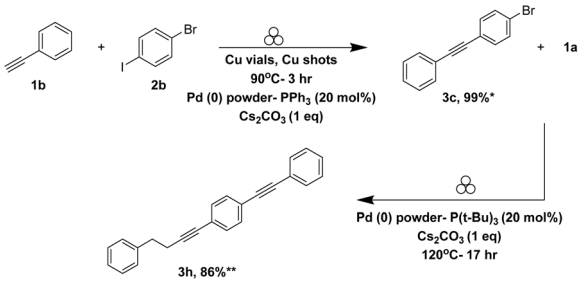

Scheme 4 Tandem one pot mechanochemical Sonogashira reaction exploiting varying reactivity of iodine and bromine substituents. reactions performed using a Cu ball (3/32″), Cu vial (2″ × 0.5″) with milling at 18 Hz using a Spex Certiprep 8000M. * Calculated as GCMS % conversion, ** Calculated as isolated yield.

observed as 99%. After milling at 90 °C for three hours, the vial was cooled before adding 4-phenyl-1-butyne (**1a**) and tri-*tert*-butylphosphine. The reaction mixture was then milled for an additional 17 hours at 120 °C, yielding 1-(4-phenylbut-1-yn-1-yl)-4-(phenylethynyl)benzene (**3h**) in 86% yield (Scheme 4).

3.3 Examining the phenomenon of Pd embedding into Cu vials

To investigate the suspected embedding of Pd within the copper milling vial surfaces, a copper vial that had been overloaded with excess Pd powder utilized in the previous synthetic utility reactions was analysed using SEM and EDS. As shown in Fig. 3, Pd contamination is apparent when compared to an unused copper vial. Contamination is confined to distinct regions of ~100 μm or more long scattered across the vial surface rather than being homogeneously distributed. The copper vials also showed trace silica-containing species (SiO_2), likely residual on the vial surface from sanding during the machining process. Phosphorus-containing species mapped surprisingly well with the Pd regions, suggesting an affinity between the two which may suggest catalyst formation responsible for promoting the reaction. Similarly, potassium-containing species also mapped well onto the Pd regions. More information on other contaminant species which are not constrained to copper or Pd regions can be found in SI 7.

To determine if the addition of 5 mol% Pd was sufficient for reliable embedding and Pd build-up on the surface over time, multiple freshly machined copper vials were used for the standard reaction. These vials were then subjected to surface analysis to confirm Pd embedding and assess its ability to form an active catalyst for C–C bond formation. Copper vial 1 was used under optimized conditions with a 5 mol% Pd powder loading, resulting in 55% conversion to the desired product (see Table 4, entry 1 and Fig. 4a). This result suggests the *in situ* formation of an active catalytic species. Subsequent surface analysis

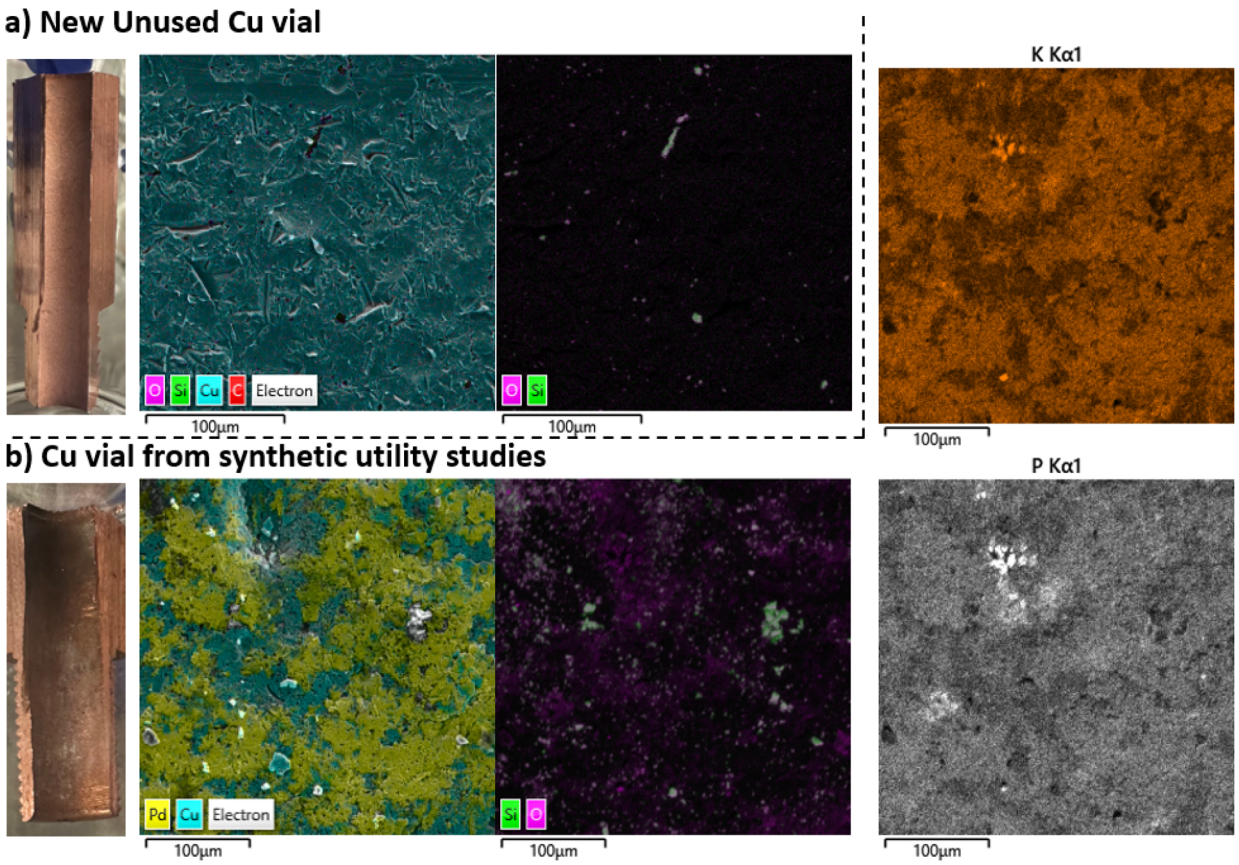

Fig. 3 SEM-EDS chemical composition maps of the elemental species on (a) a brand new, unused copper vial, and (b) a copper vial utilized for a variety of reactions to test reaction substrate scope. More composition maps of other species observed on the vial utilized for a variety of reactions are available in SI 7.

Table 4 Screening Palladium powder load for recyclability and surface analysis[a]

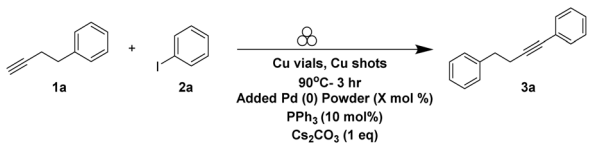

Entry	Pd (mol%)	Conversion[b] (%)	Cu vial label
1	5	55	Vial 1
2	5	57	Vial 2
3	—	5	Vial 2
4	—	3	Vial 2
5	—	27	Vial 2

[a] Reactions performed using a Cu ball (3/32″), Cu vial (2″ × 0.5″) with milling at 18 Hz and 90 °C using a Spex Certiprep 8000M. [b] % Conversion reported using GCMS.

confirmed that 5 mol% Pd was sufficient for embedding (see Fig. 4b). The Pd appears in generally smaller regions ~10–20 μm or more. These findings ensure that 5 mol% additions of Pd lead to increased reactivity in each subsequent trial rather than reduced reactivity as the amount of added Pd must be sufficient to overcome the rate of surface wear and loss to ensure high yields.

We note that the surface of the vial upon reaction completion was coated with a dark black residue (see Fig. 4a). Attempts to remove this residue by sonication in acetone, isopropanol, and ethyl acetate were unsuccessful, but citric acid was found to restore the copper to visually clean. SEM-EDS indicated that, in both clean and dirty regions, SiO_2 (from vessel sanding during manufacture) and Cs_2CO_3 are present on the surface. Surprisingly, iodine species can also be seen to cover the Cu vial surface in both regions. Regions more intensely cleaned show more uniform iodine species coverage while poorly cleaned areas show spotty iodine species coverage suggesting species are deeply incorporated into the vial (see Fig. 4b). Aside from this, there was no significant difference in the surface composition

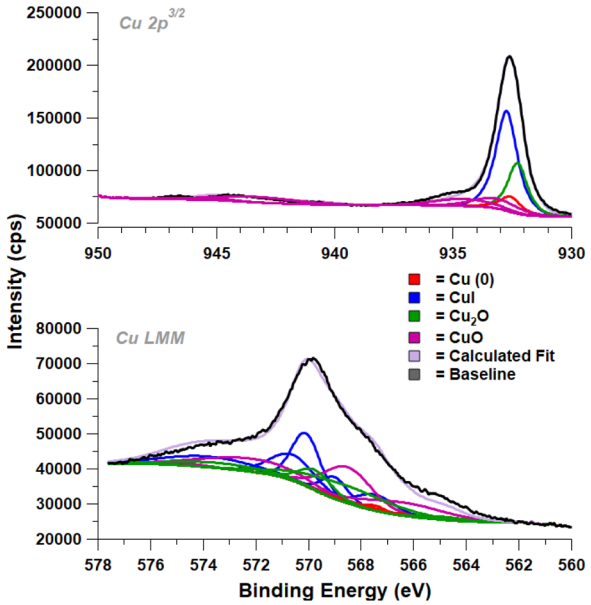

Fig. 5 XPS spectra of the clean region of vial 1 and associated fits from copper surface species.

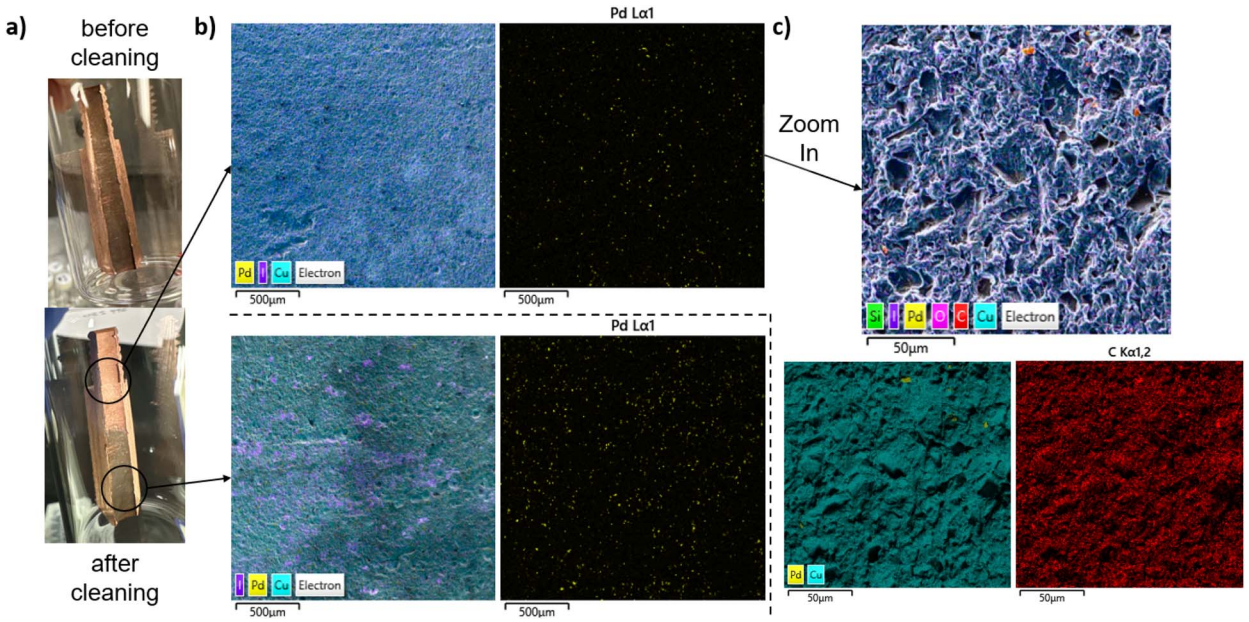

Fig. 4 (a) Optical images of vial 1 (as described in Table 4) before and after cleaning, (b) SEM-EDS chemical composition maps of significant elemental species on clean and dirty regions of vial 1, and (c) SEM-EDS chemical composition maps of significant elemental species on clean region on vial 1 zooming into the embedded Pd powder.

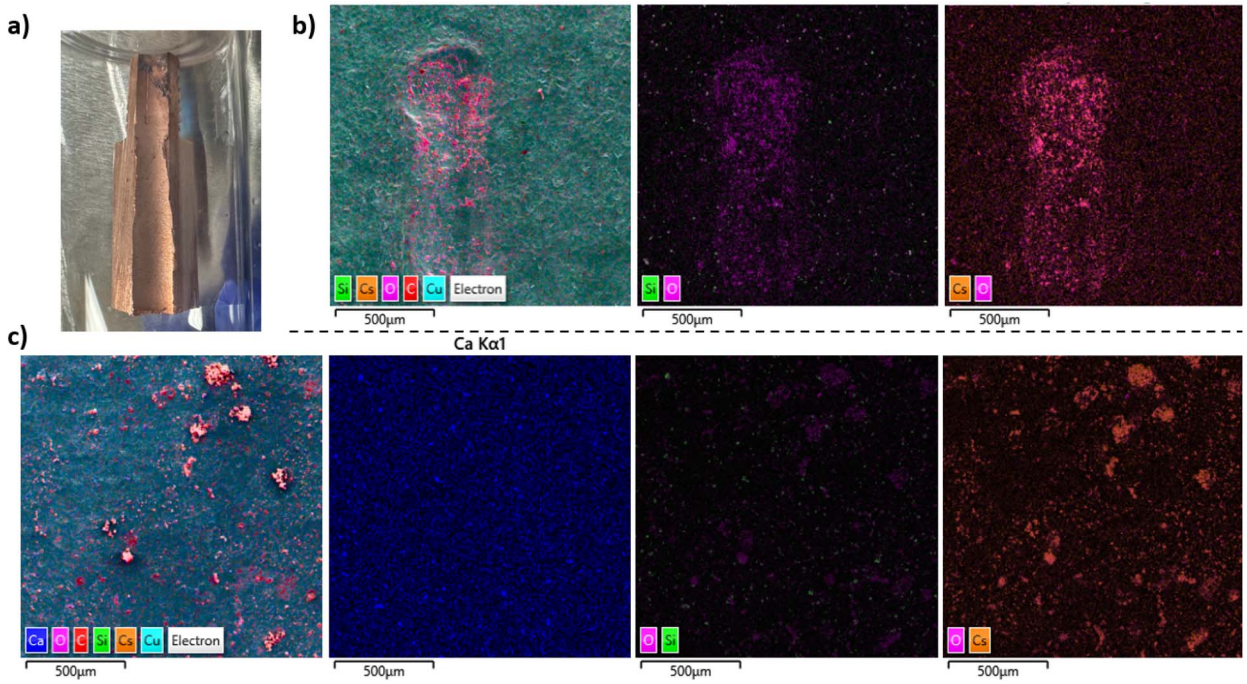

Fig. 6 (a) Vial 2 after cleaning by sonication in acetone, SEM-EDS chemical composition maps of the elemental species on (b) a scratched portion of the surface, and (c) an average area on the surface.

between the clean and dirty vial regions. Further examinations by XPS reveal that the copper reacts with the iodine from the iodobenzene (**2a**) to form CuI which accounts for the penetration of the iodine species into the surface observed by SEM (see Fig. 5, note that residual copper oxides are also observed). A more in-depth analysis of XPS data is available in SI 7.

A second freshly machined Cu vial was subjected to the same conditions with 5 mol% Pd, yielding comparable results (Table 4, entry 2). This vial was then used for three additional runs without introducing new Pd powder, leading to a progressive decline in conversion (Table 4, entries 3–5 and Fig. 6a). The small uptick noted in Table 4, entry 5 was unexpected and may be the result of the release of additional sub-surface Pd following additional milling, but this is beyond the current scope of this work. Further studies by secondary-ion mass spectrometry (SIMS) depth profiling, will aim to examine the extent of Pd embedding into the Cu vials, with reactions run for up to 5 cycles. The yield drop suggests the gradual depletion of embedded Pd, which was further corroborated by surface analysis of vial 2. SEM revealed that no Pd remained in the vial surface (see Fig. 6). Rather, the surface was covered with Cs_2CO_3 and SiO_2. Cs_2CO_3 species tended to be more concentrated in scratches on the surface. We also observed Ca species which we attribute to being present in the jar sanding matrix due to the overlap of Ca and SiO_2 species when observed (see Fig. 6 and SI 7).

4 Conclusion

In conclusion, we have demonstrated that palladium powder serves as an effective alternative to pre-formed catalysts for Sonogashira coupling under mechanochemical conditions. This system accommodates a wide variety of terminal alkynes, with temperature, ligand, base all playing crucial roles in reaction efficiency. Temperature control and ligand presence facilitate the formation of the active catalyst, while the base promotes reductive elimination *via* ion pairing.

Surface analysis confirmed that Pd progressively embeds into the copper vial over time. Using excess Pd powder results in an embedded Pd load that enables multiple reaction cycles before recharging is necessary. A 5 mol% Pd loading has been identified as sufficient to recharge the system for subsequent reactions.

Furthermore, temperature control and ligand selection enable chemoselective activation of different aryl halides over one another. Iodobenzene, with a lower thermal activation energy barrier, reacts more readily than bromobenzene. Bromobenzene, requiring a higher activation energy, necessitates a more electron-donating ligand, such as tri-*tert*-butylphosphine, and longer reaction times. By tuning temperature and proper ligand choice, selective activation of one halide over another is achievable which is not typically observed in solution-phase reactions. These findings highlight the potential of mechanochemically developed, solvent-free catalytic systems to expand the scope of metal–ligand catalysis, enabling transformations that may be challenging or impractical in conventional solution chemistry.

Author contributions

Author contributions to this work according to the CRediT standardised contribution descriptions are as follows: Sheeniza Shah (conceptualization, data curation, formal analysis,

investigation, methodology, project administration, visualization, writing – original draft), Thinh Tran (data curation, formal analysis, investigation, validation, writing – review and editing), Tim Dao (data curation, formal analysis, investigation), Alexandria Garza (data curation, formal analysis, investigation), Mennatullah Mokhtar (formal analysis, project administration, validation, visualization, writing – review and editing), Kathleen Floyd (conceptualization, data curation, formal analysis, investigation, project administration, validation, visualization, writing – review and editing), Lizette Mella (data curation, formal analysis, investigation, validation, writing – review and editing), James Batteas (conceptualization, funding acquisition, project administration, supervision, writing – review and editing), and James Mack (conceptualization, funding acquisition, project administration, supervision, writing – review and editing).

Conflicts of interest

There are no conflicts to declare.

Data availability

The data supporting this article have been included as part of the supplementary information (SI). Supplementary information: chemical details, notes on general procedures and methods, reaction optimization studies, catalyst wear and vial surface studies, and representative product verification data. See DOI: **https://doi.org/10.1039/d5mr00060b**.

Acknowledgements

The surface analysis component of this work (K. F., L. M., and J. D. B.) was supported by the NSF Center for the Mechanical Control of Chemistry (CMCC), under award number CHE-2303044. The CMCC is part of the Centers for Chemical Innovation Program in the NSF Division of Chemistry. Initial project development began under NSF award CHE-1900097, with S. S. and T. D. 100% supported by CHE-1900097. T. T. was supported 50% by the CMCC (CHE-2303044) and 50% by CHE-1900097, while M. M. was 100% supported by the CMCC. The NSF REU participant, Alexandria Garza, was 100% supported by CHE-1659648.

Notes and references

1 Q.-D. Wang, S.-X. Zhang, Z.-W. Zhang, Y. Wang, M. Ma, X.-Q. Chu and Z.-L. Shen, *Org. Lett.*, 2022, **24**, 4919–4924.
2 A. Hirsch, Acetylene Chemistry. Chemistry, Biology and Materials Science. By François Diederich, Peter J. Stang and Rik R. Tykwinski, *Angew. Chem., Int. Ed.*, 2005, **44**, 3803–3804.
3 N. Mukherjee, D. Kundu and B. C. Ranu, *Chem. Commun.*, 2014, **50**, 15784–15787.
4 J. Ma, Q. Wang, Y. Sun, E. Zhu, X. Li, H. Tan, G. Chen and C. Zheng, *Chem. Commun.*, 2023, **59**, 5043–5046.
5 A. F. Littke and G. C. Fu, *Angew. Chem., Int. Ed.*, 2002, **41**, 4176–4211.
6 R. Thorwirth, A. Stolle and B. Ondruschka, *Green Chem.*, 2010, **12**, 985–991.
7 D. A. Fulmer, W. C. Shearouse, S. T. Medonza and J. Mack, *Green Chem.*, 2009, **11**, 1821–1825.
8 W. Pickhardt, E. Siegfried, S. Fabig, M. F. Rappen, M. Etter, M. Wohlgemuth, S. Grätz and L. Borchardt, *Angew. Chem., Int. Ed.*, 2023, **62**, e202301490.
9 W. Pickhardt, C. Beaković, M. Mayer, M. Wohlgemuth, F. J. L. Kraus, M. Etter, S. Grätz and L. Borchardt, *Angew. Chem., Int. Ed.*, 2022, **61**, e202205003.
10 S. Hwang, S. Grätz and L. Borchardt, *Chem. Commun.*, 2022, **58**, 1661–1671.
11 A. C. Jones, J. A. Leitch, S. E. Raby-Buck and D. L. Browne, *Nat. Synth.*, 2022, **1**, 763–775.
12 L. Chen, D. Leslie, M. G. Coleman and J. Mack, *Chem. Sci.*, 2018, **9**, 4650–4661.
13 D. Tan, V. Štrukil, C. Mottillo and T. Friščić, *Chem. Commun.*, 2014, **50**, 5248–5250.
14 R. A. Haley, A. R. Zellner, J. A. Krause, H. Guan and J. Mack, *ACS Sustain. Chem. Eng.*, 2016, **4**, 2464–2469.
15 T. Seo, T. Ishiyama, K. Kubota and H. Ito, *Chem. Sci.*, 2019, **10**, 8202–8210.
16 R. R. A. Bolt, S. E. Raby-Buck, K. Ingram, J. A. Leitch and D. L. Browne, *Angew. Chem., Int. Ed.*, 2022, **61**(44), e202210508.
17 K. Kubota, T. Seo and H. Ito, *Faraday Discuss.*, 2023, **241**, 104–113.
18 C. G. Vogt, M. Oltermann, W. Pickhardt, S. Grätz and L. Borchardt, *Adv. Energy Sustainability Res.*, 2021, **2**, 2100011.
19 K. Kubota, T. Endo, M. Uesugi, Y. Hayashi and H. Ito, *ChemSusChem*, 2022, **15**, e202102132.
20 K. Kubota, T. Seo, K. Koide, Y. Hasegawa and H. Ito, *Nat. Commun.*, 2019, **10**, 111.
21 K. Kubota, R. Takahashi, M. Uesugi and H. Ito, *ACS Sustain. Chem. Eng.*, 2020, **8**, 16577–16582.
22 C. B. Lennox, T. H. Borchers, L. Gonnet, C. J. Barrett, S. G. Koenig, K. Nagapudi and T. Friščić, *Chem. Sci.*, 2023, **14**, 7475–7481.
23 R. H. Hastings, M. M. Mokhtar, A. Ruggles, C. Schmidt, D. Bourdeau, M. C. Haibach, H. Geneste, J. Mack, S. S. Co and I. R. Speight, *Org. Process Res. Dev.*, 2023, **27**(9), 1667–1676A.
24 W. Pickhardt, S. Grätz and L. Borchardt, *Chem.–Eur. J.*, 2020, **26**, 12903–12911.
25 Y. Gao, C. Feng, T. Seo, K. Kubota and H. Ito, *Chem. Sci.*, 2022, **13**, 430–438.
26 J. M. Andersen and H. F. Starbuck, *J. Org. Chem.*, 2021, **86**, 13983–13989.
27 M. C. Biesinger, *Surf. Interface Anal.*, 2017, **49**, 1325–1334.
28 W. A. Carole and T. J. Colacot, *Chem.–Eur. J.*, 2016, **22**, 7686–7695.
29 L. Takacs and J. S. McHenry, *J. Mater. Sci.*, 2006, **41**, 5246–5249.

30 F. Puccetti, C. Schumacher, H. Wotruba, J. G. Hernández and C. Bolm, *ACS Sustain. Chem. Eng.*, 2020, **8**, 7262–7266.
31 L. Malatesia and M. Angoletta, *J. Chem. Soc.*, 1957, 1186–1188.
32 P. W. N. M. van Leeuwen, *Homogeneous Catalysis: Understanding the Art*, Springer, Netherlands, 2004.
33 K. Kubota, R. Takahashi and H. Ito, *Chem. Sci.*, 2019, **10**, 5837–5842.
34 D. C. Waddell, T. D. Clark and J. Mack, *Tetrahedron Lett.*, 2012, **53**, 4510–4513.
35 R. Takahashi, A. Hu, P. Gao, Y. Gao, Y. Pang, T. Seo, J. Jiang, S. Maeda, H. Takaya, K. Kubota and H. Ito, *Nat. Commun.*, 2021, **12**, 6691.
36 D. R. Coulson, L. C. Satek and S. O. Grim, *Inorg. Synth.*, 1972, 121–124.
37 Tetrakis(triphenylphosphine) palladium(0), **https://www.sigmaaldrich.com/US/en/product/aldrich/697265?srsltid=AfmBOooRjmbT_2L3wfNV0Uj1k9w7wKoC2h9kX64IYntudlt_13oVAr2P**, accessed December 19th, 2024, 2024.
38 Palladium, **https://www.sigmaaldrich.com/US/en/product/aldrich/203939?srsltid=AfmBOor4OpGdkRn5UtYGQSOFOBVsOkC5omMrcSMf7z4p53ii1ftV3Rpy**, accessed December 19th, 2024, 2024.
39 Triphenylphosphine, **https://www.sigmaaldrich.com/US/en/product/mm/808270**, accessed December 19th, 2024, 2024.